Processing and Application of Ceramics 14 [3] (2020) 195–202
https://doi.org/10.2298/PAC2003195N

Evidence of magneto-electric coupling and electrical study of CFO modified BNT/BT composites

Dipika Nanda[1], Buddhadev Samanta[1], Mukesh Goel[2], Pawan Kumar[1,*]

[1]*Department of Physics, National Institute of Technology, Rourkela 769008 Odisha, India*
[2]*Department of Engineering and Maths, Sheffield Hallam University, Sheffield, S1 1WB, UK*

Received 28 January 2020; Received in revised form 23 April 2020; Accepted 16 June 2020

Abstract

(1-x)(0.93$Bi_{0.5}Na_{0.5}TiO_3$/0.07$BaTiO_3$)-x$CoFe_2O_4$ ((1-x)BNT/BT-xCFO, where x = 0.1, 0.2, 0.3, 0.4 and 0.5) composite samples were synthesized by microwave assisted solid state reaction route and sintered at 1050 °C. X-ray diffraction study showed the presence of ferroelectric/ferromagnetic (FE/FM) phases without any peak of secondary phase. This was further confirmed by SEM study showing the presence of both FE/FM grains distinctly. Frequency dependent dielectric study showed maximum dielectric constant (ε_r) for the composite sample with x = 0.4. Polarization versus electric field (P-E) loop study revealed that maximum remnant polarization ($2P_r$ = 1.75 $\mu C/cm^2$) was found also for the 0.6BNT/BT-0.4CFO sample. Remnant magnetization (M_r) of the composite sample with x = 0.4 was found to be ~7.81 emu/g. Magnetodielectric (MD) study of the 0.6BNT/BT-0.4CFO composite sample showed decrease in ε_r with the application of magnetic field and a MD effect of ~2.4% (at 10 kHz) was found. Low leakage current value (~10^{-4} A) was obtained in the 0.6BNT/BT-0.4CFO composite sample. Change in piezoresponse force microscopy contrast after poling indicated on the changes in polarization of the ferroelectric domains. Reduction in M_r, observed in magnetic force microscopy contrast gave a clear evidence of presence of electric field induced magneto-electric (ME) coupling in the 0.6BNT/BT-0.4CFO composite sample.

Keywords: *multiferroics, dielectric study, microwave processing, PFM, MFM*

I. Introduction

Multiferroic (MF) materials are attracting the attention of scientific community because of their potential use in diverge device applications and interesting physics related to coupling mechanism between ferroelectric (FE) and magnetic ordering. These materials have been well suited for applications in novel multifunctional devices, such as: multiple-state memory elements, electric-field controlled ferromagnetic (FM) resonance devices, sensors, transducers, spintronics and terahertz emitters, miniature antennas, etc. [1–4]. In order to obtain better coupling between the electric and magnetic ordering, different combinations of ferroelectric and magnetic materials have been studied, such as: i) FE-FM/AFM/FiM composites, ii) MF-FE composites, iii) MF-FM/AFM/FiM composites and iv) MF-MF composites [5,6]. Existence of ME response above room temperature remains an important parameter from application point of view.

Although single phase multiferroic materials have been studied earlier, their ME coupling coefficient is generally found to be low. In addition, if the ME coupling coefficient is found to be high in single phase multiferroic materials, it occurs only at very low temperatures, which hinders their practical applications. On the other hand, ME composites possess following advantages over single phase multiferroic materials: i) greater design flexibility, ii) ME response is several orders higher than single phase materials at room temperature, iii) magnetic and electrical properties can be tailored easily to obtain the desired output. Properties like moderate dielectric constant, spontaneous magnetization, DC conductivity etc. make ferrites (e.g. $NiFe_2O_4$, $MnFe_2O_4$, $CoFe_2O_4$) an important class of materials which are used in devices such as phase shifters, wideband absorbers, resonators, circulators, filters etc. Unlike magnetic materials (conducting in nature), ferrites

*Corresponding author: tel: +91 661 2462726,
e-mail: *pvn77@rediffmail.com, pawankumar@nitrkl.ac.in*

allow electromagnetic waves throughout the material. Thus, in ferrite based devices control of microwave propagation can be achieved by applying magnetic field. It is a well-known fact that production of high magnetic field requires bulky electromagnet which is not generally desired in the age of miniaturization. Hence, the combination of electrostrictive and magnetostrictive materials provides an advantage of using electric field as an input instead of using magnetic field which requires bulky magnets for producing high fields. When electric field is applied to ME composites, it produces mechanical deformation in the electrostrictive phase, which further produces magnetization in through magnetostrictive phenomena [7]. Selection of ferroelectric and ferromagnetic components in ME composites depends on various factors such as the Curie transition temperatures, piezoelectric properties, piezomagnetic properties, structural comparability etc. Resistivity of the magnetostrictive phase should be high in order to avoid short circuit path for the ME voltage, developed in the ME composite [7].

In the present work, new ME composites based on $CoFe_2O_4$ (CFO) ferrite as a magnetostrictive phase and $0.93Bi_{0.5}Na_{0.5}TiO_3/0.07BaTiO_3$ (BNT/BT, with morphotropic phase boundary composition) as a ferroelectric phase were synthesized by microwave assisted solid state reaction route. This study focuses basically on the morphological, ferroelectric, magnetic and magneto-dielectric properties of 0-3 particulate composites.

II. Experimental details

(1-*x*)BNT/BT-*x*CFO (*x* = 0.1, 0.2, 0.3, 0.4 and 0.5) composite samples were synthesized by microwave assisted solid-state reaction route. Two precursor powders (CFO and BNT/BT) were synthesized separately using Bi_2O_3, TiO_2, $BaCO_3$, Na_2CO_3, Fe_2O_3 and Co_2O_3 powders as starting compounds with high purity (99.99% Sigma Aldrich). The stoichiometric amounts of the starting compounds were weighed and ball-milled in acetone media with zirconia balls for 20 h. The CFO powder was calcined at 900 °C for 4 h in conventional furnace and the BNT/BT powder was calcined at 750 °C for 15 min in a microwave furnace. X-ray diffraction (XRD) study of the calcined powder was carried out by Rigaku Ultima IV X-ray diffractometer, Tokyo, Japan. Cubic structure with single phase was confirmed in case of the calcined CFO powder and rhombohedral phase was confirmed in case of the calcined BNT/BT powder.

These individually calcined BNT/BT and CFO powders were then mixed in different stoichiometric ratios corresponding to (1-*x*)BNT/BT-*x*CFO, where *x* = 0.1, 0.2, 0.3, 0.4 and 0.5. Polyvinyl alcohol binder solution (2 wt.%) was added to the composite powders and compressed into pellets of ~10 mm in diameter and ~1.5 mm in thickness, using a hydraulic press with 749 MPa pressure for 4 min. The green pellets were sintered at 1050 °C for 15 min each in air with a heating rate of 20 °C/min in microwave furnace. Optimum sintering temperature and time were selected in order to avoid melting of the samples and to obtain maximum density.

Scanning electron microscopy (SEM) was used to examine the detailed microstructure of each composite using SEM-JEOL-JSM 6480 LV. The sintered pellets were polished and then applied with silver paste on both sides followed by firing at 400 °C for 30 min for good electrode adhesion. Dielectric and magneto-dielectric studies were carried out by using LCR Meter (HIOKI) with variation of frequency (100 Hz–1 MHz) and in temperature range 25–400 °C at different frequencies. *I-V* characteristics and *P-E* hysteresis loop measurements were carried out for the composite samples using Radiant Technologies *P-E* loop tracer. *M-H* loop studies were performed in Microsense (EZ9-USA) vibrating sample magnetometer. Atomic force microscope (AFM, Multimode, Nanoscope IIIA) equipped with an external lock-in amplifier (SR-830, Stanford Research) and a function generator (FG120, Yokogawa) was used for the domain poling and imaging of local piezo-response of the composite samples. Detection of magnetic microstructures and topographic feature of the composite samples was performed by magnetic force microscopy (Ntegra Prima, NT-MDT) in Tapping/Lift modes. Magnetic field of 300 Oe was applied to the tip in downward direction before imaging the composite samples.

III. Results and discussion

3.1. X-ray diffraction study

XRD patterns of the (1-*x*)BNT/BT-*x*CFO composite samples are shown in Fig. 1. By comparing the XRD peaks of the CFO and BNT/BT parent samples with that of the composite samples, it is observed that with the increase of CFO content in BNT/BT matrix, ferrite phase

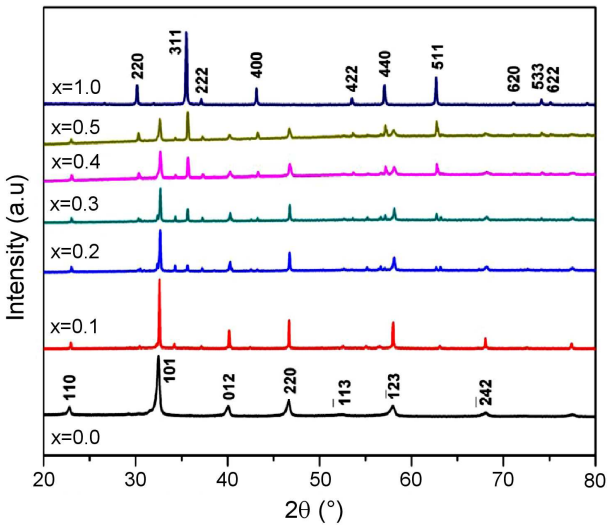

Figure 1. XRD patterns of BNT/BT, CFO and (1-*x*)BNT/BT-*x*CFO composite samples (*x* = 0.0, 0.1, 0.2, 0.3, 0.4, 0.5, 1.0)

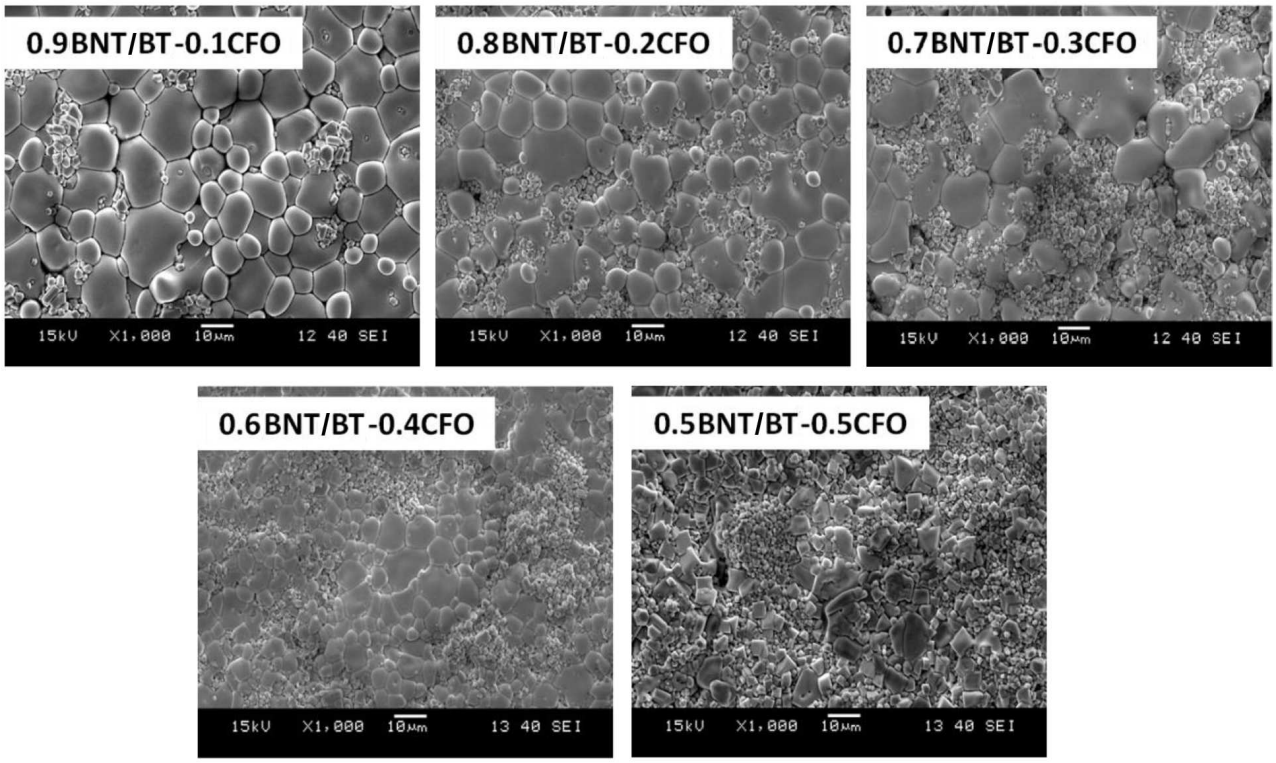

Figure 2. SEM micrographs of (1-*x*)BNT/BT-*x*CFO composite samples

peaks become distinctly visible without any secondary phase peaks. XRD patterns of the composite samples are indexed with reference to standard diffraction patterns. Present study establishes that CFO is stabilized in cubic structure and BNT/BT in rhombohedral structure in the composite samples.

3.2. Micrograph study

SEM micrographs of the (1-*x*)BNT/BT-*x*CFO composite samples are shown in Fig. 2. Two distinct phases belonging to BNT/BT and CFO can be observed in the micrographs. Smaller grains correspond to the CFO phase and larger grains correspond to the BNT/BT phase. A dense microstructure with inhomogeneous distribution of CFO grains is observed in the composite samples. The average grain size of BNT/BT phase was found to be ~3.40, 3.38, 4.22, 3.11 and 2.27 μm and the average grain size of CFO phase was found to be ~1.36, 1.18, 0.91, 0.74 and 0.42 μm for the composite samples with x = 0.1, 0.2, 0.3, 0.4 and 0.5, respectively. Experimental densities of the (1-*x*)BNT/BT-*x*CFO composite samples are listed in Table 1.

Table 1. Experimental density of (1-*x*)BNT/BT-*x*CFO composite samples

System	(1-*x*)BNT/BT-*x*CFO				
Composition, x	0.1	0.2	0.3	0.4	0.5
Density [g/cm^3]	5.59	5.57	5.58	5.60	5.48

3.3. Dielectric study

Room temperature frequency dependent dielectric spectra of the (1-*x*)BNT/BT-*x*CFO composite samples are shown in Fig. 3. Strong dispersion is observed in low frequency region, because the dipoles get enough time to align themselves along the field direction while at higher frequencies, non-availability of sufficient time results in decrease in dielectric constant (ε_r) of the composite samples. However, for the composite sample 0.6BNT/BT-0.4CFO, it is observed that in low frequency range, ε_r is the highest in comparison to other composite samples. This indicates that polarization should be greater for the 0.6BNT/BT-0.4CFO composite sample in low frequency range than other com-

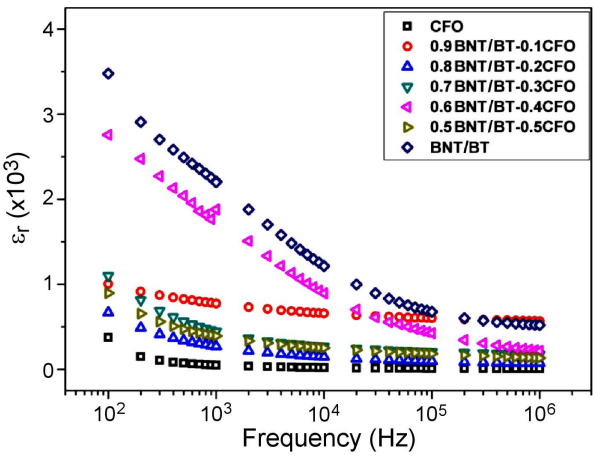

Figure 3. Frequency dependence of dielectric spectra of (1-*x*)BNT/BT-*x*CFO composite samples

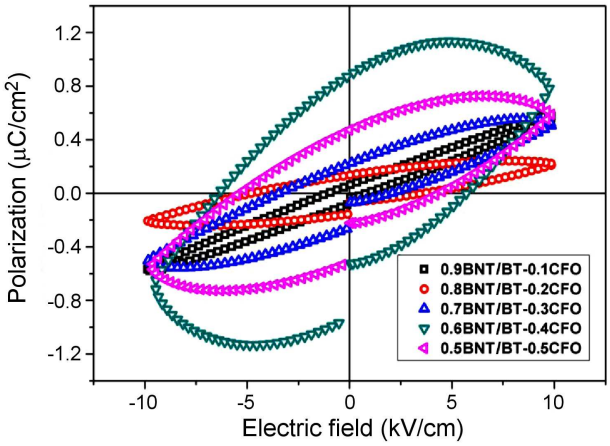

Figure 4. *P-E* loops of (1-*x*)BNT/BT-*x*CFO composite samples

posite samples, which is in well agreement with the *P-E* loop study of the composite samples (Fig. 4).

3.4. *P-E* loop study

P-E loops of the (1-*x*)BNT/BT-*x*CFO composite samples at 10 kV/cm and at frequency of 100 Hz are shown in Fig. 4. Although, the value of polarization is small, among all the compositions, the 0.6BNT/BT-0.4CFO composite sample shows a maximum $2P_s$ ~ 2.28 μC/cm^2 and $2P_r$ as ~1.75 μC/cm^2. Lower value of polarization of the composite samples may be attributed to the influence of non-ferroelectric CFO phase with relatively higher conductivity [9]. Similar observations of reduction in polarization with the addition of conductive ferrite phase in ferroelectric matrix have been reported earlier [10]. Hysteresis loops at higher fields were also attempted in order to find the saturation and remnant polarization values, but with the presence of conducting CFO phase with high leakage current, hysteresis loops turns out to be lossy in nature. Gradual broadening of *P-E* loops arises due to the increased leakage current of the composite samples [11,12]. Moreover, it is also observed that P_r increases with the increase of CFO content up to $x = 0.4$, but again decreases for the composite sample with $x = 0.5$. P_s and E_c do not follow any trend, but show maximum values for the composite sample with $x = 0.4$. Values of $2P_r$, $2P_s$ and E_c of the composite samples are given in Table 2. Leakage current of the composite sample with $x = 0.4$ was also measured and found to be very low (~ 10^{-4} A).

3.5. *M-H* loop study

Magnetization vs. magnetic field (*M-H*) loops are shown in Fig. 5a for all the composite samples, which revealed that magnetization of the composite samples increases with the increase in ferrite content. This is due to the fact that spontaneous magnetization resulting from unbalanced antiparallel spins and incorporation of ferrite content give rise to the higher number of uncompensated spins [6].

Magnetic moment of the composite samples can be calculated in terms of Bohr magneton (μ_B) as per the relation given below:

$$\eta_B = M \cdot \sigma'_S \frac{M \cdot \sigma'_S}{5585} \quad (1)$$

Table 2. Values of $2P_r$, $2P_s$ and E_c of (1-*x*)BNT/BT-*x*CFO composite samples

Composition, *x*	$2P_s$ [μC/cm^2]	$2P_r$ [μC/cm^2]	E_c [kV/cm]
0.1	1.16	0.11	0.862
0.2	0.5	0.266	4.322
0.3	1.14	0.456	2.779
0.4	2.28	1.754	6.029
0.5	1.44	0.95	4.864

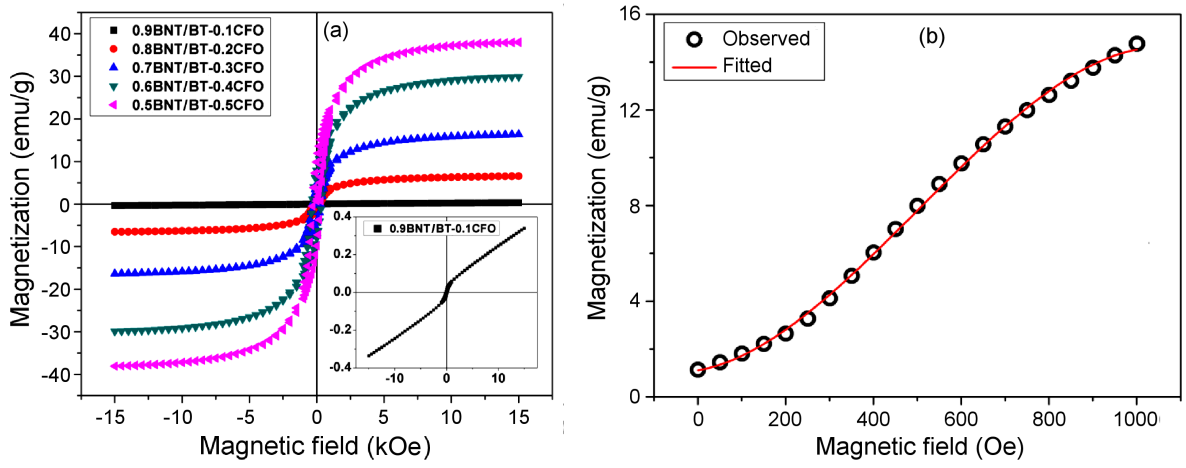

Figure 5. *M-H* loop of (1-*x*)BNT/BT-*x*CFO composite samples (a) and fitting of *M-H* loop up to 1000 Oe of the 0.6BNT/BT-0.4CFO composite sample (b)

Table 3. Values of M_s, M_r, H_c and η_B values for all composite samples

Composition, x	M_s [emu/g]	M_r [emu/g]	H_c [Oe]	η_B [μB]
0.1	0.339	0.017	144	0.013
0.2	6.443	1.488	275	0.251
0.3	16.38	4.295	305	0.644
0.4	29.91	7.815	344	1.188
0.5	38.03	9.677	298	1.525

Table 4. Spontaneous magnetization and susceptibility values with their corresponding errors of 0.6BNT/BT-0.4CFO composite sample

Equation	$M = m_0 + \chi^1 \cdot h + \chi^2 \cdot h^2 + \chi^3 \cdot h^3$	
	Value	Standard error
M_0 [emu/g]	1.100	0.113
χ^1 [emu/g Oe]	0.003	9.998×10^{-4}
χ^2 [emu/g (Oe)^2]	3.013×10^{-5}	2.354×10^{-6}
χ^3 [emu/g (Oe)^3]	-2.002×10^{-8}	1.544×10^{-9}

where M stands for molecular weight, σ'_S signifies magnetization value per gram mol of the sample and 5585 is the magnetic factor [13]. Values of M_s, M_r, coercive field (H_c) and magnetic moments η_B of all the composite samples are listed in Table 3. Maximal saturation magnetization was found for the composite sample with x = 0.5. However, our aim in this work is to have better magnetization along with good polarization value. This criterium is fulfilled for the composite sample with x = 0.4. Hence, from the *P-E* loop and *M-H* loop study, it is concluded that the 0.6BNT/BT-0.4CFO composite sample shows better polarization and magnetization properties. Consequently, further study of the composite sample with x = 0.4 is only reported. Magnetization *vs.* magnetic field curve for the composite sample with x = 0.4 was fitted up to 1000 Oe as shown in Fig. 5b in order to find theoretical susceptibility of the composite sample. Spontaneous magnetization and susceptibilities (up to third order) values with their corresponding errors are listed in Table 4.

Figure 6 shows temperature dependent dielectric spectra of the 0.6BNT/BT-0.4CFO composite sample.

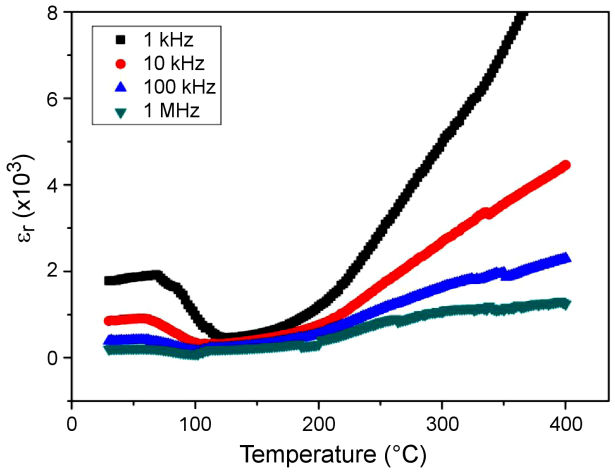

Figure 6. Temperature dependence of dielectric spectra of 0.6BNT/BT-0.4CFO composite samples

It is observed that ε_r decreases with the increase of frequency but increases with temperature. Dielectric transition ~60 °C has been reported in literatures as the depolarization temperature (T_d) of BNT/BT system where the sample undergoes a transition from ferroelectric (FE) to anti-ferroelectric (AFE) phase [14] while the relaxation behaviour ~300 °C corresponds to that of cobalt ferrite composite samples. ε_r is higher at lower frequencies due to the dominance of dipolar and interfacial polarizations hence the rate of increase of dielectric constant at 1 kHz frequency was found to be higher as compared to other frequencies.

3.6. Magneto-dielectric study

Variation of ε_r with frequency in presence of magnetic field of the 0.6BNT/BT-0.4CFO composite sample is given Fig. 7a. It has been reported that spin-pair correlation of neighbouring spins is the deciding factor for negative or positive sign of the magneto-dielectric effect [6]. It can be elaborated as when magnetic field is applied, higher number of magnetic spins gets aligned along the direction of the field resulting in disordered electric dipoles. This change in orientation of electric dipoles results in increase or decrease in dielectric constant leading to negative or positive dielectric constant. However, in our case negative MD effect was observed for the composite sample with x = 0.4. It was observed that ε_r decreases with increase in frequency as well as with increase of magnetic field. Decrease in ε_r in the presence of applied magnetic field signifies a negative coupling coefficient.

Figure 7b illustrates the variation of ε_r with magnetic field at different frequencies. It has been observed that ε_r decreases rapidly in lower field region while it remains almost unaltered after a certain field. This is due to the fact that at higher magnetic field, spins get aligned in a particular direction without any further change in their orientation, which results in very negligible change in the magnetic phase configuration. This ultimately leads to almost no change in the polarization of ferroelectric phase resulting in very small variation of dielectric con-

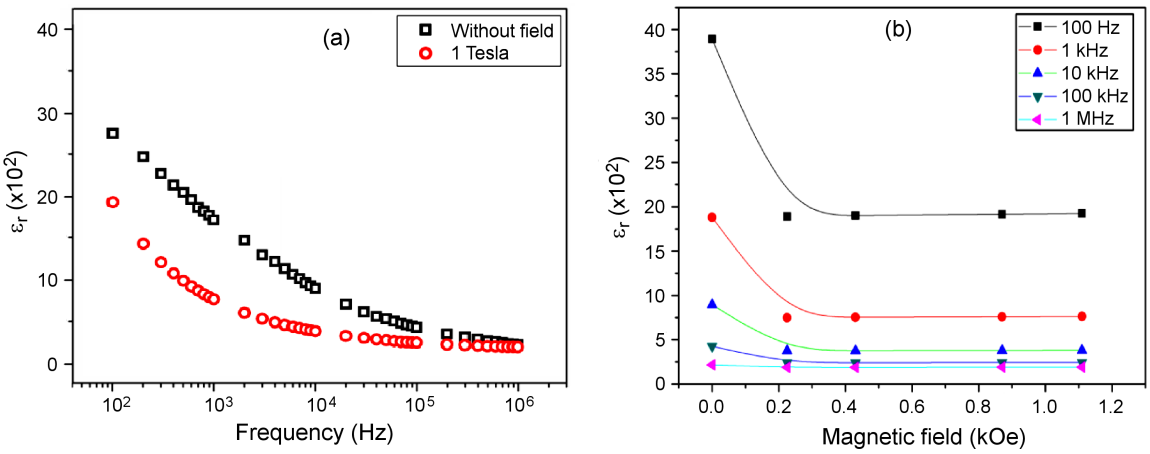

Figure 7. Variation of ε_r with frequency at magnetic field of 0 and 1 T (a) and at different magnetic fields (b) of 0.6BNT/BT-0.4CFO composite samples

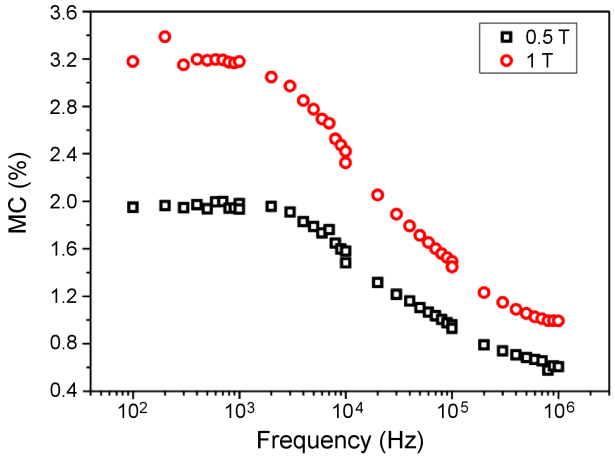

Figure 8. Variation of magneto-capacitance with frequency at magnetic field of 0.5 and 1 T of 0.6BNT/BT-0.4CFO composite sample

stant after certain magnetic field. Figure 8 represents magneto-capacitance (*MC*) *vs*. frequency at 0.5 and 1 T fields. According to the Maxwell Wagner theory, *MC* (%) can be calculated as:

$$MC = \frac{\varepsilon_r(H,T) - \varepsilon_r(0,T)}{\varepsilon_r(0,T)} \cdot 100 \qquad (2)$$

where $\varepsilon_r(H,T)$ is dielectric constant in the presence of magnetic field at temperature T, $\varepsilon_r(0,T)$ is the dielectric constant in the absence of magnetic field at temperature T. *MC* effect of ~2.4% (at 1 T) and ~1.5% (at 0.5 T) was observed at about 10 kHz frequency. Magneto-dielectric behaviour in the ME composite samples may arise due to several possible reasons, such as magneto-resistance effect, magnetostriction effect, or ME coupling [13]. *MC* follows a decreasing trend with frequency at both applied fields. Due to high temperature sintering there remains a possibility of formation of divalent or trivalent cations (such as Fe^{2+}, Fe^{3+}) in the CFO phase of the composite samples. Thus, the hopping of electrons at lower frequency becomes easier resulting in the formation of electric dipoles which again contributes to overall polarization (thus capacitance). At higher frequencies hopping becomes restricted resulting in the decrease in capacitance of the composite samples [15,16].

3.7. PFM and MFM studies

Figures 9a and 9b show PFM images (out of plane direction) of the 0.6BNT/BT-0.4CFO composite sample before and after poling, respectively. In Fig. 9a, PFM image contrast reveals the existence of randomly oriented downward polarization of domains. This is due to the fact that in a PFM image bright areas and dark areas across the surface correspond to ferroelectric domains with the polarization oriented upwards and downwards, respectively [17]. However, in the poled composite samples, as shown in Fig. 9b, clear bright contrasts are

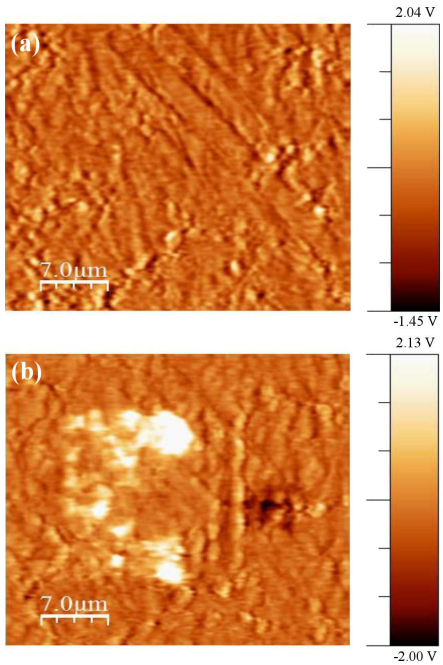

Figure 9. PFM images of 0.6BNT/BT-0.4CFO composite samples: a) before and b) after poling

observed, which indicates polarization of domains in upward direction. As shown in Fig. 9b, before poling the local coercive voltage was found to be in the range of −1.45 V to 2.04 V, whereas after poling, coercive voltage was observed in the range of −2.00 V to 2.13 V [17,18]. This increase in coercive voltage clearly implies the increase in alignment of ferroelectric domains in the same direction. This further confirms the electromechanical response of ferroelectric domains towards the externally applied voltage.

Figures 10a and 10b show MFM images of the 0.6BNT/BT-0.4CFO composite sample before and after poling, respectively. Phase shift scale provided with the MFM image gives a clear indication of effective magnetic moments in the composite samples. Marked regions show the difference in contrast before and after electrical poling of composite samples. Lighter contrast in Fig. 10b indicates increase in M_r in vertical direction (perpendicular to the sample surface) after electrical poling. This can be attributed to the fact that as CFO has negative magnetostriction [19]; magnetic moments tend to align in the in-plane direction resulting in decreased M_r in out of plane direction. Hence, dark regions in Fig. 10b indicate reduced Mr due to the compressive strain in CFO phase [19]. Since MFM is generally intended to characterize electric control of magnetism in ME composite samples, this reduction of M_r with the application of electric voltage provides a conclusive evidence of the presence of electric field induced ME coupling in the composite samples [20–22].

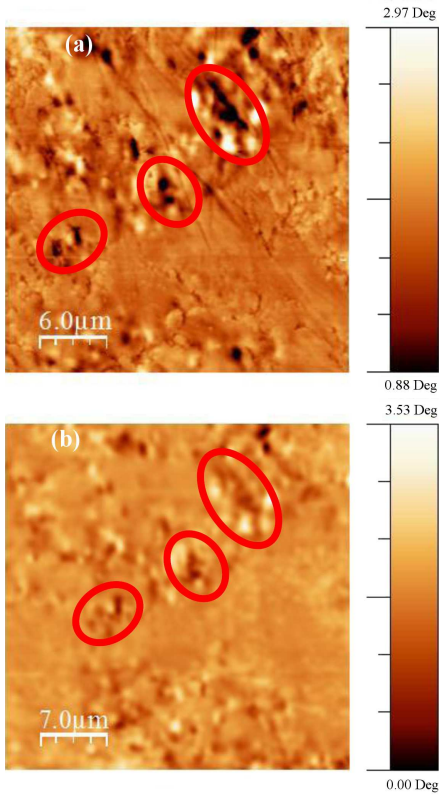

Figure 10. MFM images of 0.6BNT/BT-0.4CFO composite samples: a) before and b) after poling

IV. Conclusions

(1-x)BNT/BT-xCFO (where x = 0.1, 0.2, 0.3, 0.4, 0.5) composite samples were sintered at 1050 °C for 15 min in microwave furnace. Experimental density, ~5.60 g/cm^3 was found to be maximum for the composite sample with x = 0.4. Frequency dependent dielectric spectra revealed maximum ε_r for the composite sample with x = 0.4. M_r and μ_B for the composite sample with x = 0.4 were found to be ~7.815 emu/g and ~1.188, respectively. P_r value was found to be maximum for the composite sample with x = 0.4. Very low leakage current (~10^{-4} A) of the composite sample with x = 0.4 was observed. Magneto-dielectric study showed that ε_r decreases with the application of magnetic field and *MC* effect of ~2.4% (at 1 T) and ~1.5% (at 0.5 T) was observed at about 10 kHz frequency. Change in PFM contrast after electrical poling suggested changes in polarization of ferroelectric domains from upward to downward direction. Reduction in M_r in MFM contrast gave a clear evidence of the presence of electric field induced ME coupling in the 0.6BNT/BT-0.4CFO composite sample.

References

1. W. Eerenstein, N.D. Mathur, J.F. Scott, "Multiferroic and magnetoelectric materials", *Nature*, **442** [7104] (2006) 759–765.
2. H. Palneedi, V. Annapureddy, S. Priya, J. Ryu, "Status and perspectives of multiferroic magnetoelectric composite materials and applications", *Actuators*, **5** [1] (2016) 9.
3. M. Fiebig, "Revival of the magnetoelectric effect", *J. Phys. D. Appl. Phys.*, **38** [8] (2005) R123–R152.
4. K.F. Wang, J.M. Liu, Z.F. Ren, "Multiferroicity: The coupling between magnetic and polarization orders", *Adv. Phys.*, **58** [4] (2009) 321–448.
5. C.W. Nan, M.I. Bichurin, S. Dong, D. Viehland, G. Srinivasan, "Multiferroic magnetoelectric composites: Historical perspective, status, and future directions", *J. Appl. Phys.*, **103** [3] (2008) 031101.
6. D.K. Pradhan, V.S. Puli, S. Narayan Tripathy, D.K. Pradhan, J.F. Scott, R.S. Katiyar, "Room temperature multiferroic properties of $Pb(Fe_{0.5}Nb_{0.5})O_3$-$Co_{0.65}Zn_{0.35}Fe_2O_4$ composites", *J. Appl. Phys.*, **114** [23] (2013) 234106.
7. C.E. Ciomaga, O.G. Avadanei, I. Dumitru, M. Airimioaei, S. Tascu, F. Tufescu, L. Mitoseriu, "Engineering magnetoelectric composites towards application as tunable microwave filters", *J. Phys. D. Appl. Phys.*, **49** [12] (2016) 125002.
8. V.R. Mudinepalli, S.H. Song, M. Ravi, J.Q. Li, B.S. Murty, "Multiferroic properties of lead-free $Ni_{0.5}Zn_{0.5}Fe_{1.9}O_{4-\delta}$-$Na_{0.5}Bi_{0.5}TiO_3$ composites synthesized by spark plasma sintering", *Ceram. Int.*, **41** [5] (2015) 6882–6888.
9. K. Bala, J. Shah, N.S. Negi, R.K. Kotnala, "Induced magnetoelectric coupling and photoluminescence response in solution-processed $CoFe_2O_4$/$Pb_{0.6}Sr_{0.4}TiO_3$ multiferroic composite film", *Integr. Ferroelectr.*, **183** [1] (2017) 110–125.
10. B. Dhanalakshmi, P.S.V. Subba Rao, B. Parvatheeswara Rao, C.G. Kim, "Enhanced ferromagnetic order in Mn doped $BiFeO_3$-$Ni_{0.5}Zn_{0.5}Fe_2O_4$ multiferroic composites",

J. Nanosci. Nanotechnol., **16** [10] (2016) 11089–11093.
11. B. Dhanalakshmi, P. Kollu, C.H.W. Barnes, B. Parvatheeswara Rao, P.S.V.S. Rao, "Multiferroic and magnetoelectric studies on BMFO-NZFO nanocomposites", *Appl. Phys. A Mater. Sci. Process.*, **124** [5] (2018) 396.
12. J. Li, Y. Pu, Y. Shi, R. Shi, X. Wang, M. Yang, W. Wang, X. Guo, X. Peng, "Dielectric, multiferroic and magnetodielectric properties of (1-x)$BaTiO_3$-xSr_2CoMoO_6 solid solution", *Ceram. Int.*, **45** [13] (2019) 16353–16360.
13. N. Adhlakha, K.L. Yadav, R. Singh, "$BiFeO_3$-$CoFe_2O_4$-$PbTiO_3$ composites: Structural, multiferroic, and optical characteristics", *J. Mater. Sci.*, **50** [5] (2015) 2073–2084.
14. D. Nanda, P. Kumar, B. Samanta, R. Sahu, A. Singh, "Structural, dielectric, ferroelectric and magnetic properties of (BNT-BT)-NCZF composites synthesized by a microwave-assisted solid-state reaction route", *J. Electron. Mater.*, **48** [8] (2019) 5039–5047.
15. D.K. Pradhan, P. Misra, V.S. Puli, S. Sahoo, D.K. Pradhan, R.S. Katiyar, "Studies on structural, dielectric, and transport properties of $Ni_{0.65}Zn_{0.35}Fe_2O_4$", *J. Appl. Phys.*, **115** [24] (2014) 243904.
16. X. Chen, J. Xiao, J. Yao, Z. Kang, F. Yang, X. Zeng, "Room temperature magnetoelectric coupling study in multiferroic $Bi_4NdTi_3Fe_{0.7}Ni_{0.3}O_{15}$ prepared by a multi-calcination procedure", *Ceram. Int.*, **40** [5] (2014) 6815–6819.
17. G. Caruntu, A. Yourdkhani, M. Vopsaroiu, G. Srinivasan, "Probing the local strain-mediated magnetoelectric coupling in multiferroic nanocomposites by magnetic field-assisted piezoresponse force microscopy", *Nanoscale*, **4** [10] (2012) 3218–3227.
18. F. Zhang, Q. Miao, G. Tian, Z. Lu, L. Zhao, H. Fan, X. Song, Z. Li, M. Zeng, X. Gao, "Unique nano-domain structures in self-assembled $BiFeO_3$ and $Pb(Zr,Ti)O_3$ ferroelectric nanocapacitors", *Nanotechnology*, **27** [1] (2015) 015703.
19. Z. Wang, R. Viswan, B. Hu, J.F. Li, V.G. Harris, D. Viehland, "Domain rotation induced strain effect on the magnetic and magneto-electric response in $CoFe_2O_4$/$Pb(Mg,Nb)O_3$-$PbTiO_3$ heterostructures", *J. Appl. Phys.*, **111** [3] (2012) 034108.
20. B.G. Kim, J.Y. Son, C.H. Kim, J.H. Cho, "Kelvin probe force microscopy study of multiferroic $BiMnO_3$ thin film for high-density nonvolatile storage devices", *J. Korean Phys. Soc.*, **46** [1] (2005) 33–36.
21. R. Rai, M.A. Valente, I. Bdikin, A.L. Kholkin, S. Sharma, "Enhanced ferroelectric and magnetic properties of perovskite structured $Bi_{1-x-y}Gd_xLa_yFe_{1-y}Ti_yO_3$ magnetoelectric ceramics", *J. Phys. Chem. Solids*, **74** [7] (2013) 905–912.
22. C. Liu, J. Ma, J. Ma, Y. Zhang, J. Chen, C.W. Nan, "Cautions to predicate multiferroic by atomic force microscopy", *AIP Adv.*, **7** [5] (2017) 055003.